

Fig. 2 Example of a trajectory showing the similarity between the density and impedance profiles in the region of the fallopian canal (bony canal surrounding the facial nerve). In the top, an arbitrary CT slice along the trajectory is depicted

Conclusion

Electrical impedance could be a potential marker to enhance overall system's safety during image-guided robotic cochlear implantation. An example of using this technique could be by combining it with drilling forces to further increase reliability of an existing pose estimation algorithm [2]. To further develop and verify this technique we propose to investigate integrated impedance sensing during continuous drilling into the mastoid.

References

- [1] Bell B, Gerber N, Williamson T, et al. (2013) In Vitro Accuracy Evaluation of Image-Guided Robot System for Direct Cochlear Access. *Otology & Neurotology* 34: 1284–1290
- [2] Williamson T, Bell B, Gerber N, et al. (2013) Estimation of tool pose based on force-density correlation during robotic drilling. *IEEE Transactions Biomedical Engineering* 60: 969–76
- [3] Ansó J, Dür C, Gavaghan K, et al. (2015) A Neuromonitoring Approach to Facial Nerve Preservation During Image-guided Robotic Cochlear Implantation. *Otology & Neurotology* (37): 89–98
- [4] Dai Y, Xue Y, Zhang J, (2013) Drilling Electrode for Real-Time Measurement of Electrical Impedance in Bone Tissues. *Annals Biomedical Engineering* 42(3):1–10
- [5] Bolger C, Carozzo C, Roger T, et al. (2006) A preliminary study of reliability of impedance measurement to detect iatrogenic initial pedicle perforation. *Europe Spine Journal* 15:316–320

Electrode array insertion for minimally invasive robotic cochlear implantation with a guide tube

W. Wimmer^{1,2}, K. Gavaghan³, T. Williamson³, N. Gerber¹, M. Caversaccio^{1,2}, S. Weber³

¹University of Bern, Artificial Hearing Research, ARTORG Center, Bern, Switzerland

²Inselspital Bern, Department of Otolaryngology, Head and Neck Surgery, Bern, Switzerland

³University of Bern, Image-Guided Therapy, ARTORG Center, Bern, Switzerland

Keywords Direct cochlear access · CI insertion models · Thiel vs. Formalin · Cochlear duct length

Purpose

Minimally invasive robotic cochlear implantation demands an adapted surgical procedure when compared with conventional cochlear implant (CI) surgery. During insertion, the visibility and maneuverability of the electrode array is limited because of the small size of the direct cochlear access (DCA) tunnel (1.8 mm in diameter). It has previously been shown that a manual insertion of CI electrode arrays is feasible by introducing a tympanomeatal flap as an auxiliary access to the middle ear cavity [1]. To further reduce the invasiveness of the implantation procedure, i.e. to avoid the tympanomeatal flap, an insertion guide tube was developed to bypass the middle ear cavity and to enable a direct insertion of the array from the mastoid surface through the DCA tunnel. The aim of this ex vivo study was to evaluate the new implantation procedure for clinical applicability.

Methods

An insertion guide tube prototype that resembles the shape of the DCA drill was manufactured. It consists of 2 parts to enable removal after array insertion. Sixteen temporal bone specimens (8 Thiel fixed and 8 Formalin fixed) were prepared by placement of 4 fiducial landmark screws. Preoperative CT imaging was performed and drill trajectories were planned to align with the center of the round window. A high-accuracy robotic system was used to drill DCA tunnels (1.8 mm in diameter) in the temporal bones [2]. Free-fitting electrode arrays (28 mm length) were marked to achieve an angular insertion depth of 540° as calculated from the cochlear size of each specimen [3]. Manual insertion from the mastoid surface through the round window was performed through the insertion guide tube (Fig. 1). After insertion was complete, the guide tube was removed and the electrode lead was fixed. Postoperative cone beam CT and microCT imaging was performed to evaluate the insertion outcome.

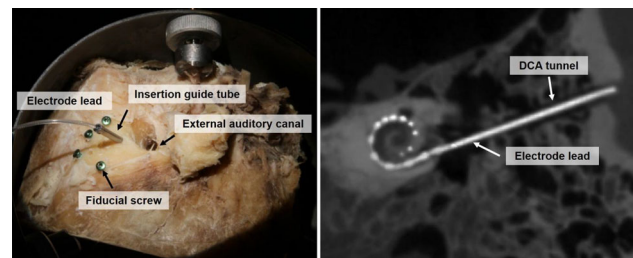


Fig. 1 (Left) Formalin fixed temporal bone with insertion guide tube and inserted CI electrode array. (Right) Postoperative pseudocoronal cone beam CT slice showing the implantation outcome in a Formalin fixed temporal bone

Results

In all specimens the direct CI array insertions from the mastoid surface into the cochlea were feasible without complications using the guide tube. The removal of the insertion guide tube was possible without retracting the inserted arrays. One minor problem was the visualization of the insertion depth marks on the arrays at the level of the round window. All electrode arrays ($n = 16$) were inserted into the scala tympani, with an average angular insertion depth of 538° (Thiel fixed) and 409° (Formalin fixed). The arrays inserted into Thiel specimens showed a smooth array course, whereas in 4 Formalin specimens bending of the electrode array at the hook region occurred.

Conclusion

The presented results show that CI array insertion through a removable guide tube seems to be feasible. The insertion guide tube serves as a base for further improvements of the implantation strategy. Further efforts must additionally consider a suitable method for sealing the electrode array after insertion and the management unforeseen events, such as bleeding or CSF leakage. The cochlear size based estimation of the insertion depths yielded promising results, however, must be evaluated in a clinical setting. Our results further indicate that Formalin fixed specimens are limited models for deep array insertions.

References

- [1] Wimmer W, Bell B, Huth ME, Weisstanner C, Gerber N, Kompis M, Weber S, Caversaccio M (2014) Cone beam and micro-computed tomography validation of manual array insertion for minimally invasive cochlear implantation., *Audiol. Neurootol.*, vol. 19, pp. 22–30
- [2] Bell B, Gerber N, Williamson T, Gavaghan K, Wimmer W, Caversaccio M, Weber S, (2013) In Vitro Accuracy Evaluation of Image-Guided Robot System for Direct Cochlear Access., *Otol. Neurotol.*, vol. 34, pp. 1284–1290
- [3] Wimmer W, Bell B, Dhanasingh A, Jolly C, Weber S, Kompis M, Caversaccio M Cochlear duct length estimation: adaptation of Escude's equation, 13th international conference on cochlear implants and other implantable auditory technologies, Munich, Germany

Fully automatic determination of proximal femur morphological parameters and modeling of medullary canal

Y. Wang¹, L. Xu¹, X. Chen¹, Z. Taylor², A. F. Frangi², H. Zhang³, L. Wang³

¹Shanghai Jiao Tong University, School of Mechanical Engineering, Shanghai, China

²Center for Computational Imaging and Simulation Technologies in Biomedicine, School of University of Sheffield, Sheffield, Great Britain

³Shanghai Jiao Tong University, School of Medicine, Shanghai, China

Keywords Femoral medullary canal · Semi-spherical searching · Proximal axis · Femoral isthmus

Purpose

Total hip arthroplasty and intramedullary nailing fixation have become the most successful surgical interventions among the orthopedic community. Accurate preoperative morphological measurements of the femoral intramedullary canal are an essential part of the preoperative plan and facilitate the selection or design of the most suitable femoral implant [1,2]. Traditional measurement methods of femoral morphology are primarily based on two-dimensional images, such as anterior-posterior X-ray films. Compared to 2D measurement methods, analyzing detailed osseous morphology of the femoral canal in 3D space should be a more accurate approach [3]. This study established an automatic method of measuring the morphological parameters and medullary canal modeling.

Methods

The processing and image rendering tools of the software are based on the open-source libraries Insight Toolkit and Visualization Toolkit. The proposed automatic computation is shown in Fig. 1. A surface

model of femur is taken as an input. To automatically locate an initial seed position, a rough shape of femur should be estimated. The femur center O_f , orientation \mathbf{n}_f and femur length L are determined by its oriented bounding box. Then a plane passing through O_f with normal vector \mathbf{n}_f is used to cut mid-diaphysis of the femur. The initial seed O is located at the mass center of the section contour to begin searching along $\mathbf{n} = \mathbf{n}_f$. In each iterative step, the seed moves from the middle of the femur to the proximal end. The next optimal seed position is selected from a point set S in which every point satisfies a semi-spherical equation $OP = r$, $\mathbf{p} \cdot \mathbf{n} < 0$, where r is the step length and \mathbf{p} is the direction vector from O to P . The points can be ordered by their minimum distance R to the surface of the medullary canal. The point P_{opt} with largest R becomes the next seed position O . If the seed reach end of the femur approximately $OO_f > L/3$ searching stop. If not, continue semi-spherical searching. At the end of iteration, a centerline and a list of corresponding radii are obtained to create a center tube.

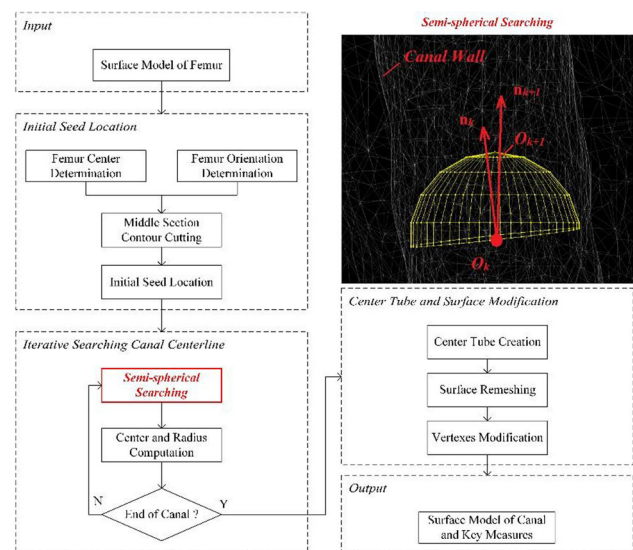


Fig. 1 The automatic computation pipeline and semi-spherical searching algorithm

After the canal tube modeling, many key morphological parameters of the proximal femur can be easily accessed. The femoral isthmus locates at the tube section with minimum radius. From tube center points, a least-squares line is fitted to represent the femoral axis and a least-squares arc is fitted to represent the femoral arch.

Results

For the method evaluation experiments, the right femur was chosen. High-resolution computed tomography studies of 88 normal people (mean age of 43 ± 27 years, 51 male, and 37 female) receiving pelvic scans for reasons not related to orthopedic conditions were selected from our institution's database. The average time cost for the entire algorithm procedure on standard computers was 1.085 s. To estimate the reliability of this method, 16 subjects (8 male and 8 female) were randomly selected from our main data set, and three trials were independently performed by three raters on all subjects. Average intra-class correlation coefficient scores were 0.9998, with a 95 % confidence interval of 0.9996 to 0.9999, indicating a robust performance (Fig. 2).